



Phenazine-based colorimetric and fluorescent sensor for the selective detection of cyanides based on supramolecular self-assembly in aqueous solution



Hai-Li Zhang, Tai-Bao Wei, Wen-Ting Li, Wen-Juan Qu, Yan-Li Leng, Jian-Hui Zhang, Qi Lin, You-Ming Zhang*, Hong Yao

Key Laboratory of Eco-Environment-Related Polymer Materials, Ministry of Education of China, Key Laboratory of Polymer Materials of Gansu Province, College of Chemistry and Chemical Engineering, Northwest Normal University, Lanzhou, Gansu 730070, PR China

ARTICLE INFO

Article history:

Received 27 July 2016

Received in revised form 25 November 2016

Accepted 14 December 2016

Available online 15 December 2016

Keywords:

Deprotonating

Cyanide sensor

Self-assembly

Dual-channel

ABSTRACT

Taking advantages of both the well-known phenazine structure and the mechanism of the supramolecular self-assembly and deprotonation process, the fluorescent and colorimetric sensor (**ZL**) was designed and synthesized, behaving as a circulation utilization (above 10 times) receptor for selective detection of cyanide anion (CN^-) in aqueous media. Upon the addition of CN^- , the sensor displayed obvious color changes from yellow to jacinth by naked eyes and the fluorescence immediately quenched (<10 s). With respect to other common anions, the sensor possessed high selectivity and sensitivity ($0.05 \mu\text{M}$) for cyanide anions. In addition, the test strips of **ZL** were fabricated, which could serve as practical colorimetric and fluorescent sensor for “in-the-field” measurements.

© 2016 Elsevier B.V. All rights reserved.

1. Introduction

The self-assembly of molecules has drawn much attention for its ability to generate excellent optical properties, which is potentially useful for ion and molecular identification [1]. Typical driving forces for the self-assembly are hydrogen bonding, π - π stacking, polar-nonpolar and charge transfer [2]. Phenazine and its derivatives could easily form the self-assembly of π -conjugated system owing to their big rigid structure [3]. The π -cores of phenazine derivatives will tune certain properties when they were modified by the amino, dialkylamino, hydroxy, nitro and other functional groups [4]. Therefore, they often were used to recognize ions and neutral molecular for these properties [5]. Meanwhile, they also are important and versatile building blocks which have been extensively designed to develop the sensors and biosensors over the years [6].

As a highly toxic anion, cyanide (CN^-) has drawn strong interest due to its harmful to environment and human body but the indispensability of chemical industry [7]. Even trace amounts of cyanide might result in extremely damage to many biological functions, such as leading to vomiting, convulsion, loss of consciousness, and eventual death [8]. The maximum acceptable level of cyanide in drinking water is only $1.9 \mu\text{M}$ by the World Health Organization (WHO) [9]. However, the release of cyanide is unavoidable for that it was widely used in many chemical processes

[10]. Therefore, there is special interest in the development of easy and affordable methods for highly selective and sensitive detection of cyanide anion [11]. Many manners have been proposed to detect cyanide, for example, chromatography [12], electrochemical [13], and titrimetric [14]. Among all these manners, fluorescence spectrometry and naked-eye detection methods are particularly attractive due to their easier operation, low cost, high sensitivity and selectivity [15].

Considering all these aspects and also as a part of our research interest in molecular recognition [16]. We synthesized a phenazine derivative **ZL** (Scheme 1), which could high sensitivity and selectivity CN^- based on the fluorescent and colorimetric dual-channel in aqueous solution. After addition of the CN^- , with the deprotonation process occurring, the intermolecular hydrogen bonds were broken and then the supramolecular self-assembly was disintegrated. It appeared a remarkable ON-OFF type fluorescent signaling behavior and an obvious color changes. Meanwhile, other common anions had no influence on the response of CN^- . This sensor also served as a recyclable component in sensing materials and the test strips were fabricated, which could be treated as a convenient and efficient CN^- test for on-site and at real-time measurement.

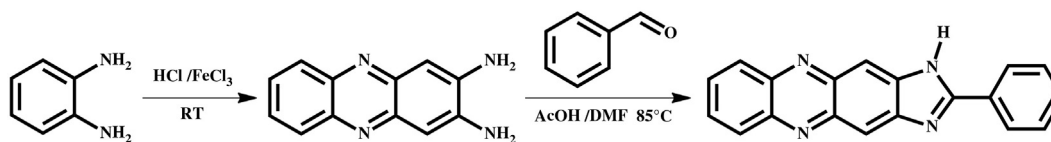
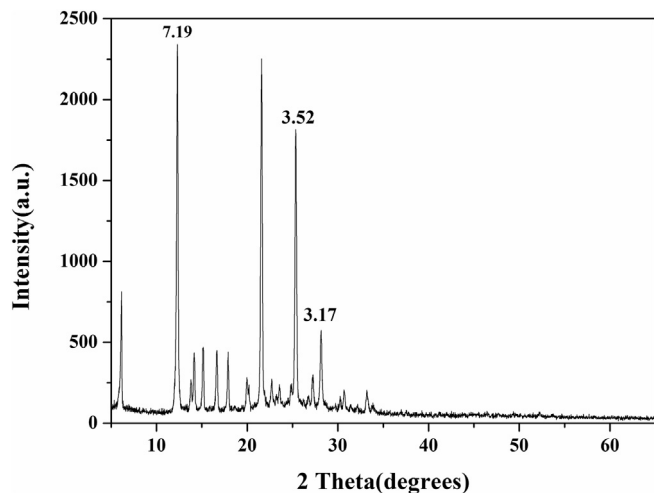
2. Experimental Section

2.1. Materials and Physical Methods

All reagents and solvents were commercially available at analytical grade and were used without further purification. ^1H NMR and ^{13}C

* Corresponding author.

E-mail addresses: weitaobao@126.com (T.-B. Wei), zhangwnwu@126.com (Y.-M. Zhang).

Scheme 1. Synthetic procedures for receptor **ZL**.Fig. 1. XRD diagram of **ZL**.

NMR spectra were recorded at a Mercury-400BB spectrometer at 400 MHz. Chemical shifts are reported in ppm downfield from tetramethylsilane (TMS, δ scale with solvent resonances as internal standards) Melting points were measured on an X-4 digital melting-point apparatus (uncorrected). Infrared spectra were performed on a Digilab FTS-3000 FT-IR spectrophotometer.

2.2. General Procedure for UV-Vis Experiments

All UV-vis spectroscopy was carried out just after the addition of tetrabutylammonium salt of anions (F^- , Cl^- , Br^- , I^- , AcO^- , $H_2PO_4^-$, HSO_4^- and ClO_4^-) and sodium salt of anions (CN^- , N_3^- , HS^- , S^{2-} , NO_2^- and SCN^-) in DMSO/ H_2O (7:3, v/v) solution, while keeping the ligand concentration constant (2.0×10^{-5} M) on a Shimadzu UV-2550 spectrometer.

2.3. General Procedure for Fluorescence Spectra Experiments

All fluorescence spectroscopy was carried out just after the addition of tetrabutylammonium salt of anions (F^- , Cl^- , Br^- , I^- , AcO^- , $H_2PO_4^-$, HSO_4^- and ClO_4^-) and sodium salt of anions (CN^- , N_3^- , HS^- , S^{2-} , NO_2^- and SCN^-) in DMSO/ H_2O (7:3, v/v) solution, while keeping the ligand concentration constant (2.0×10^{-5} M) on a Shimadzu RF-5301 spectrometer.

2.4. General Procedure for 1H NMR Experiments

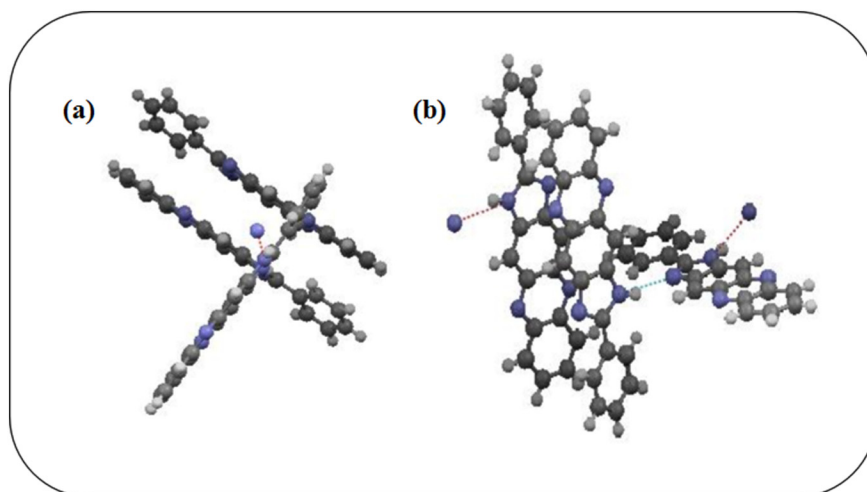
For 1H NMR titrations, the sensor of stock solutions was prepared in DMSO- d_6 , the cyanide anion was prepared in D_2O . Aliquots of the two solutions were mixed directly in NMR tubes.

2.5. Synthesis of **ZL**

2,3-Diaminophenazine (0.42 g, 2.0 mmol), benzaldehyde (0.233 g, 2.2 mmol) and five drops acetic acid (AcOH) were combined in 85 °C absolute DMF (20 ml) (Scheme 1). The solution was stirred and reflux for 8 h, after cooling to room temperature, the brown precipitate was filtrated, washed with hot absolute ethanol three times, and then re-crystallized with DMF to get brown powdery product **ZL**. The TGA (thermogravimetric analysis, N_2) revealed that **ZL** had a remarkable thermal stability, with nearly weight loss observed within 300 °C (Fig. S10).

ZL: yield: 80%; m.p. > 300 °C; 1H NMR (DMSO- d_6 , 600 MHz) δ 13.45 (s 1H), 8.52 (s 1H), 8.38–8.37 (d 2H), 8.26–8.23 (d 3H), 7.89–7.88 (d 2H), 7.67–7.66 (d 3H). ^{13}C NMR (DMSO- d_6 , 150 MHz) δ 159.90, 149.25, 142.25, 142.08, 140.88, 140.86, 140.62, 140.23, 132.22, 130.16, 129.87, 129.86, 129.60, 129.43, 129.23, 128.18, 115.23, 109.87, 106.29; IR (KBr cm^{-1}) v: 3115 (N–H), 1693 (C = N); ESI-MS m/z ($M + H^+$) Calcd for $C_{19}H_{12}N_4$ 296.1135; Found 297.114.

To better investigate the reaction mechanism of **ZL** and CN^- , we achieved the assembling structure of **ZL** from the X-ray diffraction (XRD) and the crystal structure (Figs. 1 and 2). We obtained a d-spacing of 3.51 Å by $2\theta = 25.33^\circ$ from the XRD, it suggesting that it existed π - π

Fig. 2. Different perspectives of **ZL**'s crystal structure.

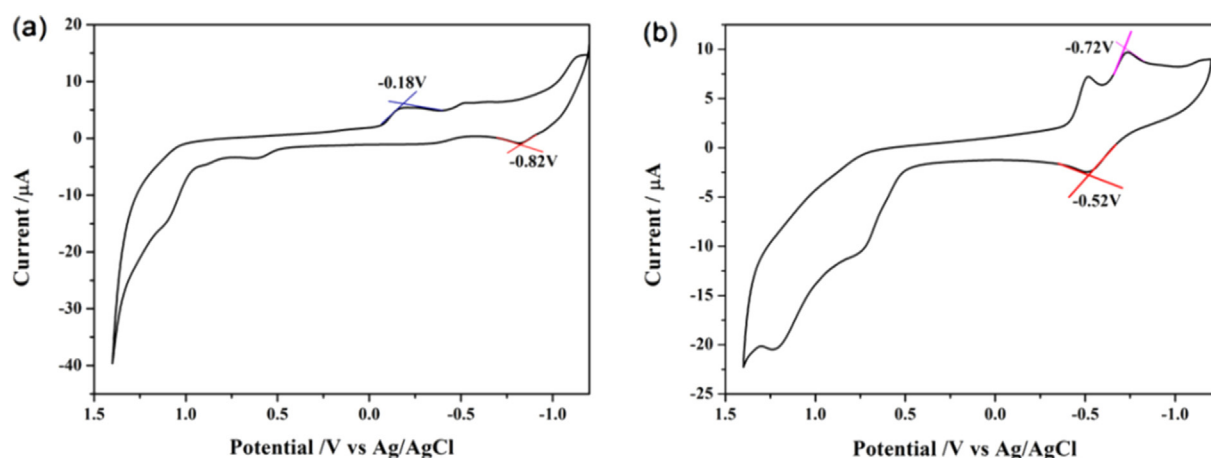


Fig. 3. Cyclic voltammetry curves of **ZL** (a) and **ZL** + CN^- (b) in DMSO solution containing 0.1 M NaNO_3 electrolyte. Scanning rate: 50 mV/s.

Table 1

Electrochemical properties of **ZL** and **ZL** + CN^- .

Compounds	$E_{\text{onset}}^{\text{oxd}}$ (V) ^a	$E_{\text{onset}}^{\text{red}}$ (V) ^a	LUMO (eV) ^b	HOMO (eV) ^c	λ_{max} /nm ^d
ZL	-0.82	-0.18	-4.22	-3.58	402
ZL + CN^-	-0.52	-0.72	-3.68	-3.88	428

^a Obtained from CV curves in NaNO_3 .

^b $E_{\text{LUMO}} = -e(4.40 - E_{\text{red}}^{\text{onset}})$ eV.

^c $E_{\text{HOMO}} = -e(4.40 - E_{\text{oxd}}^{\text{onset}})$ eV.

^d Determined in DMSO/ H_2O (7:3, v/v) solution.

stacking between molecular of **ZL**. Meanwhile, the crystal structure gave us valuable information on the assembly according to image contrast across the sample. The π -cores align antiparallel with phenazine group placed nearly parallel to the π -surface while the other side group pointed away from the π -surface. Imine nitrogen in the imidazole core are hydrogen-bonded to tertiary amine in the imidazole at another molecular. The amazing corresponding of the X-ray diffraction (XRD)

and the crystal structure provided strongly evidence for the proposal of mechanism.

The CV (cyclic voltammetry) curves of **ZL** and **ZL** + CN^- were researched in DMSO (with 0.1 M NaNO_3) using Ag/AgCl as reference electrode (Fig. 3 and Table 1). The two dissolved compounds showed different redox behaviors at the same testing conditions. The onset oxidation potentials for **ZL** and **ZL** + CN^- were -0.82 V and -0.52 V, which consistent with the HOMO energy levels of -3.58 eV and 3.88 eV respectively by the equation $E_{\text{HOMO}} = -[4.4 + E_{\text{oxd}}^{\text{onset}}]$ eV. The onset reduction potentials of **ZL** and **ZL** + CN^- were -0.18 and -0.72 eV, which consistent with the LUMO energy levels of -4.22 and -3.68 eV according to the equation $E_{\text{LUMO}} = -[4.4 + E_{\text{red}}^{\text{onset}}]$ eV [17]. At the same time, based on the equation $E_{\text{gap}} = E_{\text{LUMO}} - E_{\text{HOMO}}$ eV, we worked out the bandgap energy (E_{gap}) of **ZL** and **ZL** + CN^- were -0.65 and -0.2 eV respectively, which correspond to the red shifts at the UV-vis spectra. This study also indicated that **ZL** + CN^- could show better stability in electronic devices than **ZL**.

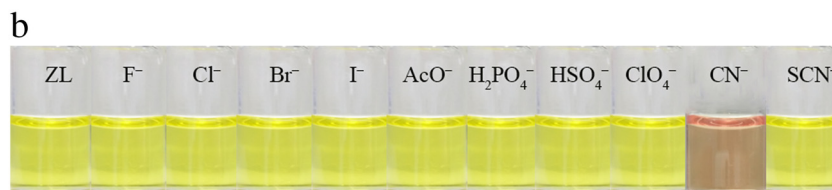
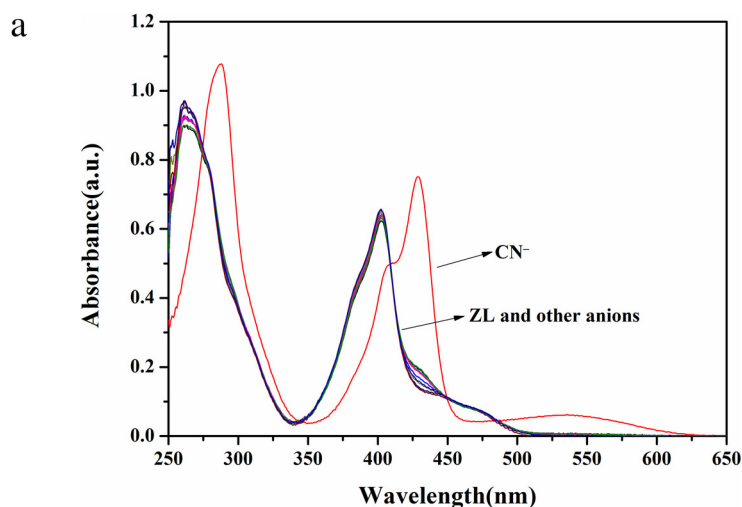


Fig. 4. (a) Absorbance spectra of **ZL** upon the addition of different anions (F^- , Cl^- , Br^- , I^- , AcO^- , H_2PO_4^- , HSO_4^- , ClO_4^- , CN^- and SCN^-) in DMSO/ H_2O (7:3, v/v) solutions. (b) Color changes of **ZL** with various anions.

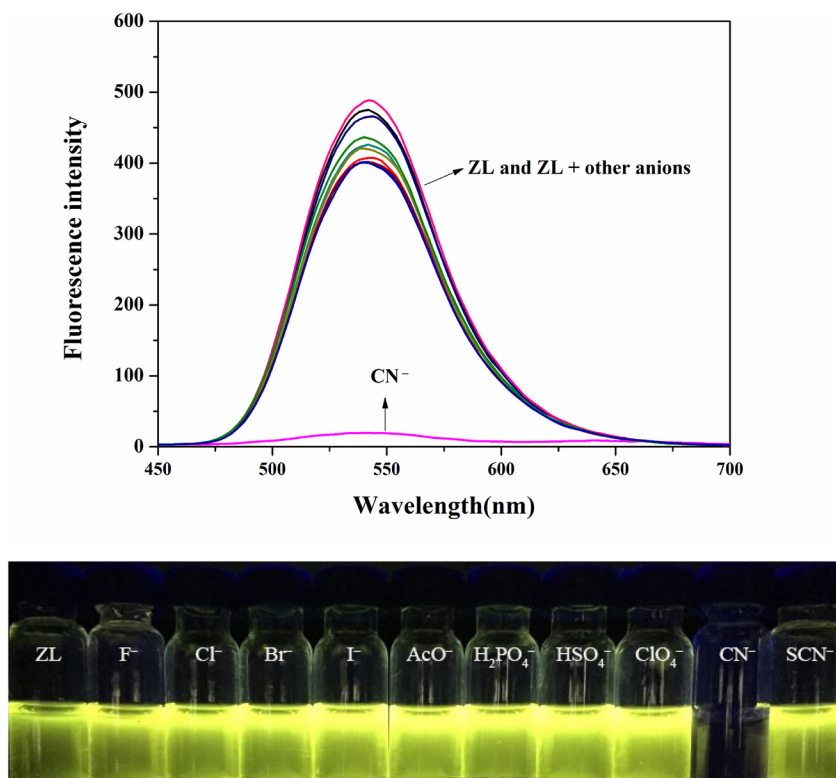


Fig. 5. (a) Fluorescent spectra of **ZL** upon the addition of different anions (F^- , Cl^- , Br^- , I^- , AcO^- , H_2PO_4^- , HSO_4^- , ClO_4^- , CN^- and SCN^-) in DMSO/ H_2O (7:3, v/v) solutions. (b) Color changes of **ZL** with various anions.

We carried out a series of recognition experiments to study its special recognition ability. The colorimetric and fluorescent sensing abilities were primarily investigated by adding various anions to the DMSO/ H_2O solution (7:3, v/v). As shown in Fig. 4b, the sensor immediately responded with obvious color changes (from yellow to jacinth) when CN^- was added to the **ZL** solution. In the corresponding UV-vis spectra, the absorbance peak at 402 nm was red shift to 428 nm (Fig. 4a). As shown in Fig. 5a, a yellow fluorescence at 542 nm appeared when the solution of sensor **ZL** was excited at 403 nm. Upon the addition of CN^- , the fluorescence emission remarkably decreased (Fig. 5b). However, when other anions solution (including F^- , Cl^- , Br^- , I^- , AcO^- , H_2PO_4^- , HSO_4^- , ClO_4^- and SCN^-) were added to the sensor **ZL**

solution, neither significant color or fluorescence change was observed. All these facts might indicate that **ZL** occurred a deprotonation process after addition of the CN^- , which broken the intermolecular hydrogen bonds and then bringing to disintegrating of the supramolecular self-assembly. The facts also confirmed that **ZL** can be capable of selectivity and sensitivity detection CN^- in DMSO/ H_2O (7:3, v/v) solution (Fig. 6).

Achieving high selectivity for the analyte of interest over a complex background of potentially competing species was a challenging task in sensor development. Fig. 5, Fig. 7 and Fig. S4 illustrated the fluorescence and UV-vis response of compound **ZL** to CN^- in the presence of other anions (F^- , Cl^- , Br^- , I^- , AcO^- , H_2PO_4^- , HSO_4^- , ClO_4^- , N_3^- , HS^- , S^{2-} , NO_2^- , and SCN^-) in DMSO/ H_2O (7:3, v/v) solution. Form the bar

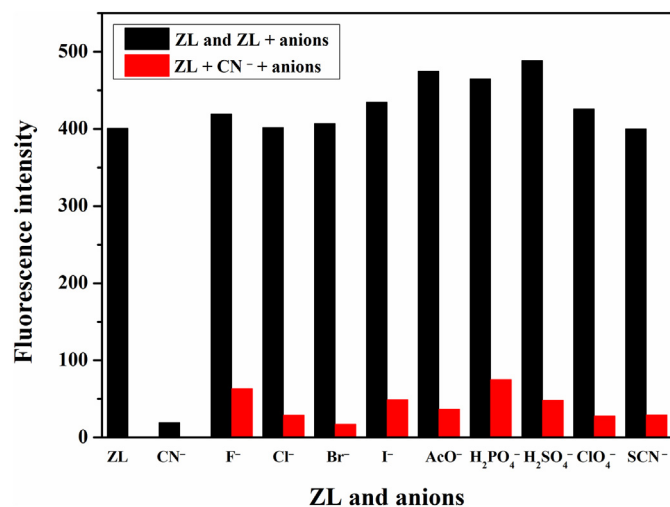


Fig. 6. Fluorescent spectra of **ZL** and **ZL**- CN^- in the presence of 50 equivalents of various anions in DMSO/ H_2O (7:3, v/v) solution ($\lambda_{\text{ex}} = 403$ nm).

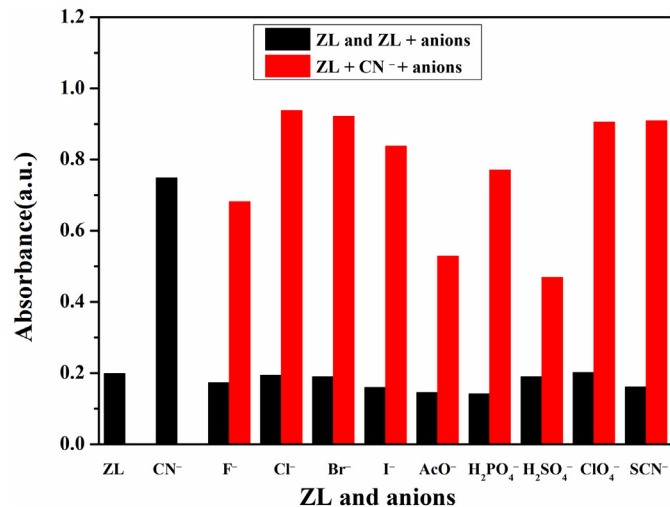


Fig. 7. UV-vis spectra of **ZL** and **ZL**- CN^- in the presence of 50 equivalents of various anions in DMSO/ H_2O (7:3, v/v) solution ($\lambda = 428$ nm).

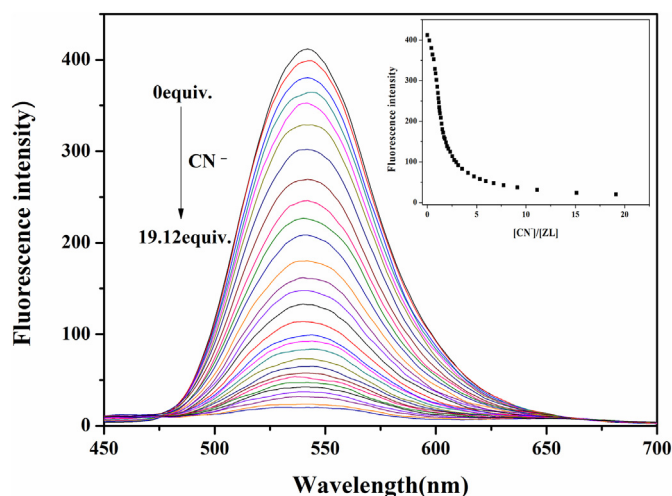


Fig. 8. Fluorescence spectra of **ZL** in the presence of different concentrations of CN^- in DMSO/ H_2O (7:3, v/v) solution. Insert: a plot of fluorescence intensity depending on the concentration of CN^- in the range from 0 to 19.12 equivalents ($\lambda_{\text{ex}} = 403 \text{ nm}$).

diagram, we could easily consider that the effects on emission and absorption intensity of **ZL** and CN^- solutions upon addition of various anions were almost negligible. Therefore, it was clear that other ions' interference were negligible small during the detection of CN^- . These results further suggested that **ZL** could be used as a sensor for CN^- over a wide range of anions.

Fluorescence and UV–vis titration were performed to gain insight into the recognition properties of receptor **ZL** as CN^- sensor. In fluorescence spectrum (Fig. 8), upon addition CN^- to receptor **ZL**, the emission at 542 nm gradually decreased. Concomitantly, in UV–vis spectra (Fig. 9), with the gradual addition of CN^- , the absorption at 402 nm decreased; while the absorption at 428 nm increased until it reached a limiting value. Moreover the presence of one isosbestic point at 408 nm indicated that sensor **ZL** reacted with cyanide anions.

The colorimetric and fluorometric detection limits of sensor **ZL** for CN^- were also tested. As shown in Fig. S5 and Fig. S6, the change of fluorescence intensity and absorbance intensity ratio were linear with increasing CN^- concentration. The detection of **ZL** for CN^- calculated on the basis of $3\sigma/m$ [18] were $7.0 \times 10^{-8} \text{ M}$ for fluorescence and $5.0 \times 10^{-8} \text{ M}$ for absorption spectra change respectively, which are both far lower than the index of WHO for CN^- in drinking water

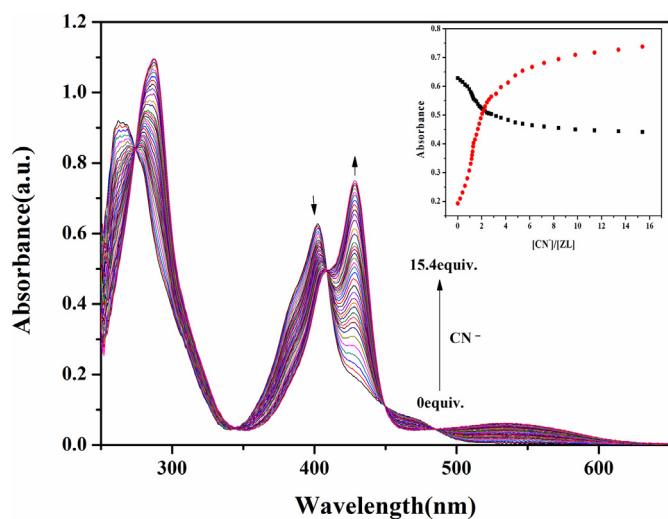


Fig. 9. UV–vis spectra of **ZL** in the presence of different concentrations of CN^- in DMSO/ H_2O (7:3, v/v) solution. Insert: a plot of absorbance depending on the concentration of CN^- in the range from 0 to 15.14 equivalents respectively at 402 nm and 428 nm.

($< 1.9 \times 10^{-6} \text{ M}$). This result also showed **ZL** has higher sensitive for cyanide anion compared with other reported CN^- sensors (Table S1).

To further investigate the reaction mechanism, ^1H NMR titration, was used to illustrate the characteristic structural changes occurring upon interaction with CN^- . As shown in Fig. S3, the ^1H NMR chemical shifts of **ZL** shown a strong peaks at 13.45 ppm, which could be assigned to the N–H proton. After addition of 0.1 equivalent of CN^- , the N–H peak at 13.45 ppm disappeared. At the same time, the other proton signals from 7.60 to 8.60 ppm have a significant upfield shift. Thus, we can indicate that cyanide could take the H proton away via deprotonating from the –NH moiety of **ZL** causing the intermolecular hydrogen bond disruption and the supramolecular self-assembly disintegration, which lead to the fluorescent quenched and the absorbance peak red shift.

In order to quantify the reaction ratio between **ZL** and CN^- , the fluorescent Job's plot (Fig. S2) was conducted by varying the concentration of both the receptor and the CN^- ion. The break point appears at the mole fraction of 0.5 which indicates the reaction ratio of **ZL** and CN^- is 1:1. It was further confirmed by the appearance of a peak at m/z 297.11 and m/z 295.14 which can be assignable to $[\text{ZL} + \text{H}^+]$ and $[\text{ZL} - \text{H}^+]$ in the ESI-MS (Fig. S1 and Fig. 10).

Above all of these tests, we rationally inferred the reaction mechanism is that the self-assembly which containing the intermolecular hydrogen bonds and π – π stacking of phenazine cores was destroyed after added CN^- by the deprotonating process (Fig. 11).

The reversibility of the sensor function was tested by addition of HClO_4 to the cyanide-sensor complex. Impressively, upon addition of HClO_4 , CN^- was removed from the **ZL**– CN^- complex and the fluorescence intensity recovered to the original strength. With addition of CN^- to the **ZL**– CN^- – HClO_4 complex, the fluorescence intensity sharply decreased (Fig. 12). The fluorescence emission of the tested solution performed alternate quenching and reviving processes with addition of CN^- and HClO_4 in turn.

The pH value of system is often considered as a significant influence factor on interactions. As shown in Fig. 13, **ZL**– CN^- was nearly non fluorescence from pH 8–13, and the fluorescence intensity was drop markedly at pH = 7. Therefore, the sensor can available for a wide pH range of 7.0–13.0 to detect CN^- .

To investigate the practical application of **ZL**, we made a comparison test strips. Test strips were prepared by immersing filter paper into a DMSO solution of **ZL** ($2 \times 10^{-5} \text{ M}$) and then drying them in air. As shown in Fig. 14, when CN^- was added on the test kits, the obvious fluorescence quenched was observed. Therefore, the test strips could conveniently detect.

3. Conclusion

In summary, we have designed and synthesized the fluorescent and colorimetric sensor **ZL** for reversible recognition cyanide ions with the supramolecular self-assembly and the deprotonation mechanism in aqueous solution. Taking advantage of the outstanding competitive ability and high sensitivity than other sensors, this work provided a novel approach for the selective recognition of CN^- . Thus, this work might stimulate the scientist interest for exploring new sensors based on the supramolecular self-assembly mechanism. Taking advantage of the recyclable of **ZL**, wide pH range application and the successful application in paper testing, we believe that the test strips could act as a convenient and efficient CN^- test kits.

Acknowledgment

This work was supported by the National Natural Science Foundation of China (nos. 21161018; 21262032; 21574104), the Program for Chang Jiang Scholars and Innovative Research Team in University of Ministry of Education of China (no. IRT1177).

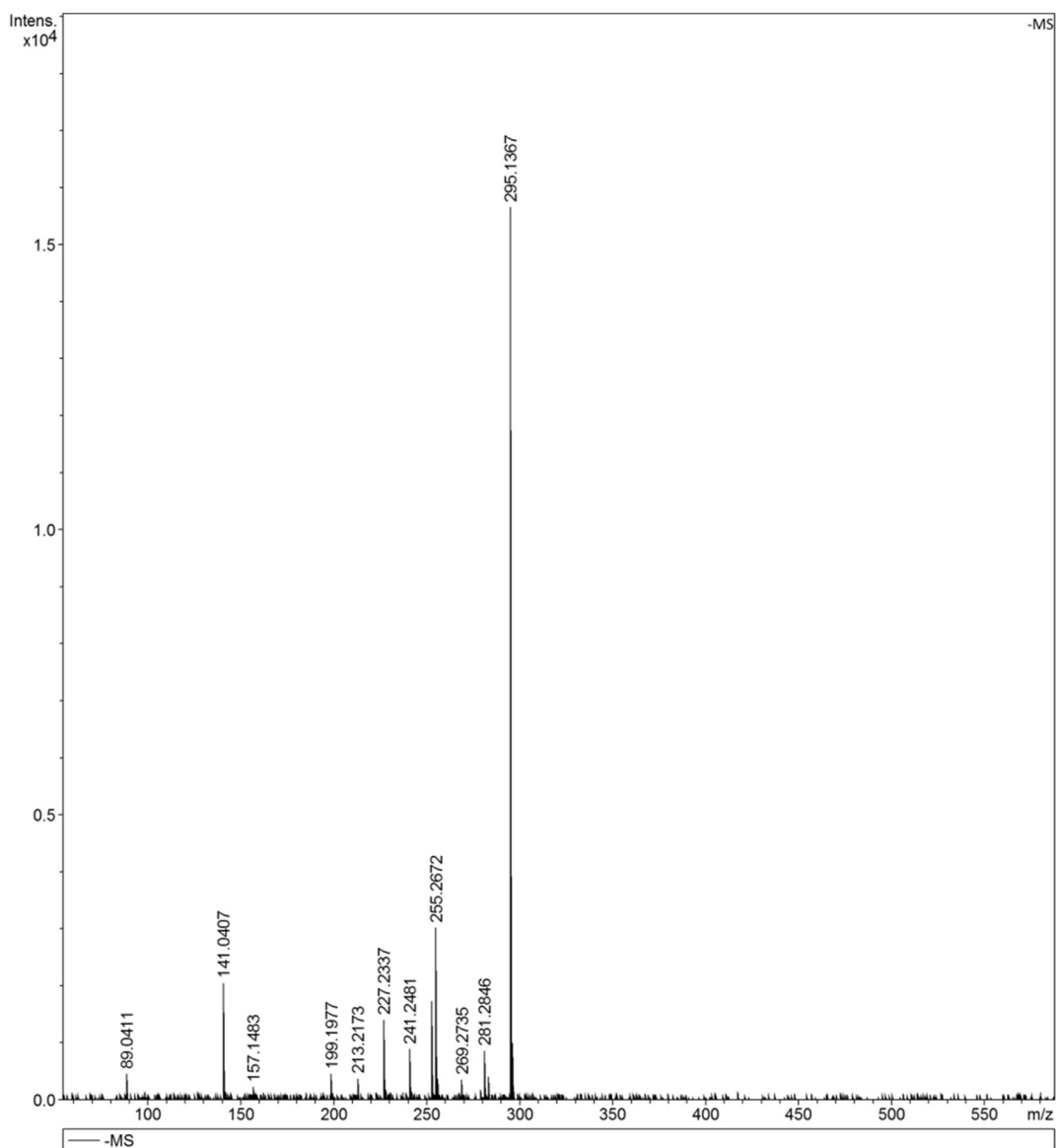


Fig. 10. The ESI-MS of ZL-CN⁻.

Appendix A. Supplementary data

Supplementary data to this article can be found online at <http://dx.doi.org/10.1016/j.saa.2016.12.022>.

References

- [1] (a) M.J.E. Resendiz, J.C. Noveron, H. Disteldorf, S. Fischer, P.J. Stang, *Org. Lett.* 6 (2004) 651–653; (b) W.J. Yuan, L. Huang, Q.Q. Zhou, G.Q. Shi, *ACS Appl. Mater. Interfaces* 6 (2014) 17003–17008.
- [2] X. Zarate, E. Schott, *RSC Adv.* 4 (2014) 15642–15649.
- [3] (a) D.C. Lee, B. Cao, K. Jang, P.M. Forster, *J. Mater. Chem.* 20 (2010) 867–873; (b) V.S.S. Mosali, G.A. Bowmaker, M. Gerard, P.A. Kilmartin, J.T. Sejdich, Z.D. Zujovcib, *Polym. Int.* 64 (2015) 1135–1141; (c) S. Biradar, Y. Shigemitsu, Y. Kubota, K. Funabiki, H. Satoh, M. Matsui, *RSC Adv.* 4 (2014) 59387–59396; (d) J.F. Zhao, Y. Liu, J.B. Soh, Y.X. Li, R. Ganguly, K.Q. Ye, F. Huo, L. Huang, A.I.Y. Tok, J.S.C. Loo, Q. Zhang, *Tetrahedron Lett.* 53 (2012) 6044–6047; (e) J. Zhao, G. Li, C. Wang, W. Chen, S.C.J. Loo, Q. Zhang, *RSC Adv.* 3 (2013) 9653–9657.
- [4] C.J. Tonzola, M.M. Alam, W. Kaminsky, S.A. Jenekhe, *J. Am. Chem. Soc.* 125 (2003) 13548–13558.
- [5] (a) F.J. Huo, J. Su, Y.Q. Sun, C.X. Yin, J.B. Chao, *Chem. Lett.* 39 (2010) 738–740; (b) Y.A. Son, Y.M. Park, S.Y. Park, C.J. Shin, S.H. Kim, *Dyes Pigments* 73 (2007) 76–80; (c) J. Xu, S.B. Sun, Q. Li, Y. Yue, Y.D. Li, S.J. Shao, *Anal. Chim. Acta* 849 (2014) 36–42; (d) F.J. Huo, C.X. Yin, Y.T. Yang, J. Su, J.B. Chao, D.S. Liu, *Anal. Chem.* 84 (2012) 2219–2223; (e) S. Erdemir, O. Kocyigit, *Sensors Actuators B* 221 (2015) 900–905; (f) C.J. Gao, X.J. Jin, X.H. Yan, P. An, Y. Zhang, L.L. Liu, H. Tian, W.S. Liu, X.J. Yao, Y. Tang, *Sensors Actuators B* 176 (2013) 775–781.
- [6] (a) J.Y. Hu, R. Liu, X.L. Zhu, X. Cai, H.J. Zhu, *Chin. Chem. Lett.* 26 (2015) 339–342; (b) C.Y. Wang, G. Li, Q.C. Zhang, *Tetrahedron Lett.* 54 (2013) 2633–2636; (c) S.M.S. Chauhan, T. Bisht, B. Garg, *Tetrahedron Lett.* 49 (2008) 6646–6649; (d) B.B. Shi, K.C. Jie, Y.J. Zhou, J. Zhou, D.Y. Xia, F.H. Huang, *J. Am. Chem. Soc.* 138 (2016) 80–83; (e) J. Li, Q. Zhang, *ACS Appl. Mater. Interfaces* 7 (2015) 28049–28062; (f) P.Y. Gu, Z.L. Wang, Q. Zhang, *J. Mater. Chem. B* 4 (2016) 7060–7074.
- [7] (a) K.W. Kulig, Atlanta. (1991); (b) S.S. Sun, A.J. Lees, *Chem. Commun.* 36 (2000) 1687–1688; (c) J. Li, J. Gao, W.W. Xiong, P.Z. Li, H. Zhang, Y. Zhao, Q. Zhang, *Chem. Asian. J.* 9 (2014) 121–125.
- [8] (a) P. Anzenbacher Jr., D.S. Tyson, K. Jursíková, F.N. Castellano, *J. Am. Chem. Soc.* 124 (2002) 6232–6233; (b) R. Koenig, *Science* 287 (2000) 1737–1738.
- [9] Guidelines for Drinking-Water Quality, World Health Organization, Geneva 12 (2011) 342–344.
- [10] Q. Zhang, J. Zhang, H.J. Zuo, C.Y. Wang, Y.J. Shen, *Tetrahedron* 72 (2016) 1244–1248.
- [11] X.B. Cheng, H. Li, F. Zheng, Q. Lin, Y.M. Zhang, H. Yao, T.B. Wei, *Dyes Pigments* 127 (2016) 59–66.
- [12] A. Safavi, N. Maleki, H.R. Shahbaazi, *Anal. Chim. Acta* 503 (2004) 213–221.
- [13] Y.G. Timofeyenko, J.J. Rosentreter, S. Mayo, *Anal. Chem.* 79 (2007) 251–255.

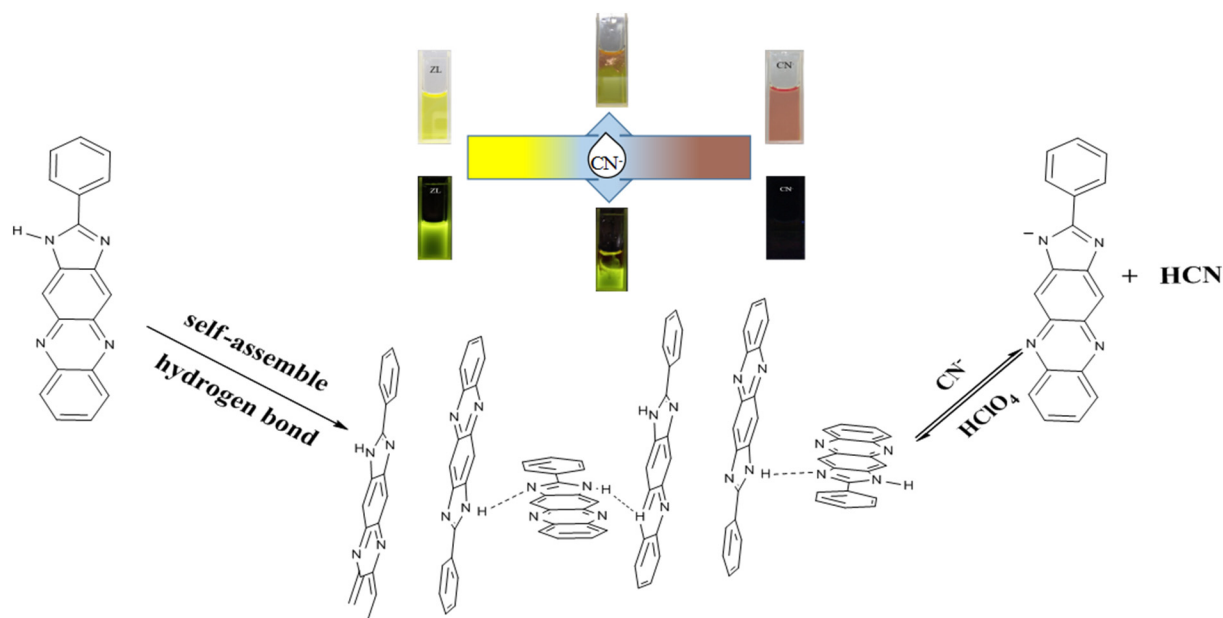


Fig. 11. The possible sensing mechanism of ZL reaction with CN^- .

- [14] P.J. Anzenbacher, D.S. Tyson, K. Jursikova, F.N. Castellano, *J. Am. Chem. Soc.* 124 (2002) 6232–6233.
- [15] (a) S.T. Wang, Y.W. Sie, C.F. Wan, A.T. Wu, *J. Lumin.* 173 (2016) 25–29;
 (b) J.J. Li, W. Wei, X.L. Qi, G.C. Zuo, J.K. Fang, W. Dong, *Sensors Actuators B* 228 (2016) 330–334;
 (c) H.J. Lee, H.J. Kim, *Tetrahedron Lett.* 53 (2012) 5455–5457.
- [16] (a) Y.M. Zhang, Q. Lin, T.B. Wei, X.P. Qin, Y. Li, *Chem. Commun.* 45 (2009) 6074–6083;
 (b) Q. Lin, X. Liu, T.B. Wei, Y.M. Zhang, *Chem. Asian. J.* 8 (2013) 3015–3021;
 (c) B.B. Shi, P. Zhang, T.B. Wei, H. Yao, Q. Lin, Y.M. Zhang, *Chem. Commun.* 49 (2013) 781–7814;
 (d) H.B. Yu, Q. Zhao, Z. Jiang, J.G. Qin, Z. Li, *Sensors Actuators B* 148 (2010) 110–116;
 (e) Q. Zeng, P. Cai, Z. Li, J.G. Qin, B.Z. Tang, *Chem. Commun.* 9 (2008) 1094–1096.
- [17] (a) G. Li, Y. Wu, J. Gao, J. Li, Y. Zhao, Q. Zhang, *Chem. Asian. J.* 8 (2013) 1574–1578;
 (b) G. Li, Y. Wu, J. Gao, C. Wang, J. Li, H. Zhang, Y. Zhao, Y. Zhao, Q. Zhang, *J. Am. Chem. Soc.* 134 (2012) 20298–20301.
- [18] Analytical Methods Committee, *Analyst* 112 (1987) 199–204.

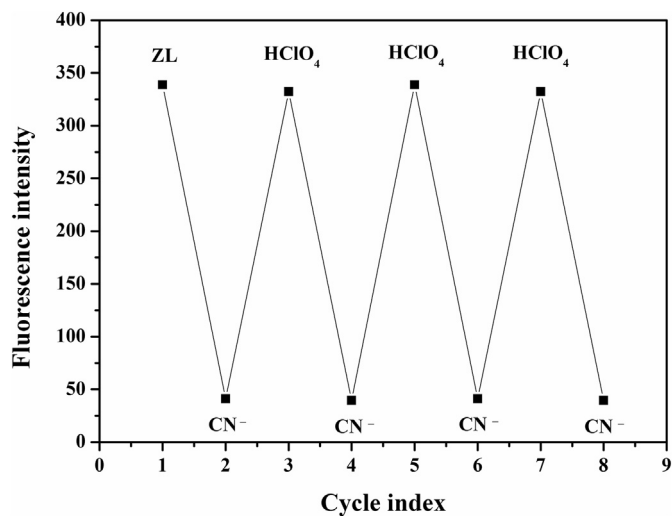


Fig. 12. The emission spectra showing the reversible complex between ZL- CN^- and HClO_4 .

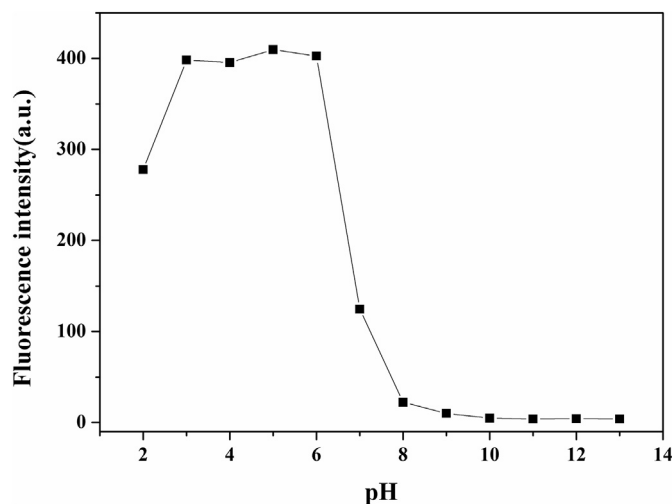


Fig. 13. ZL- CN^- in DMSO/ H_2O (7:3, v/v) at different pH values.

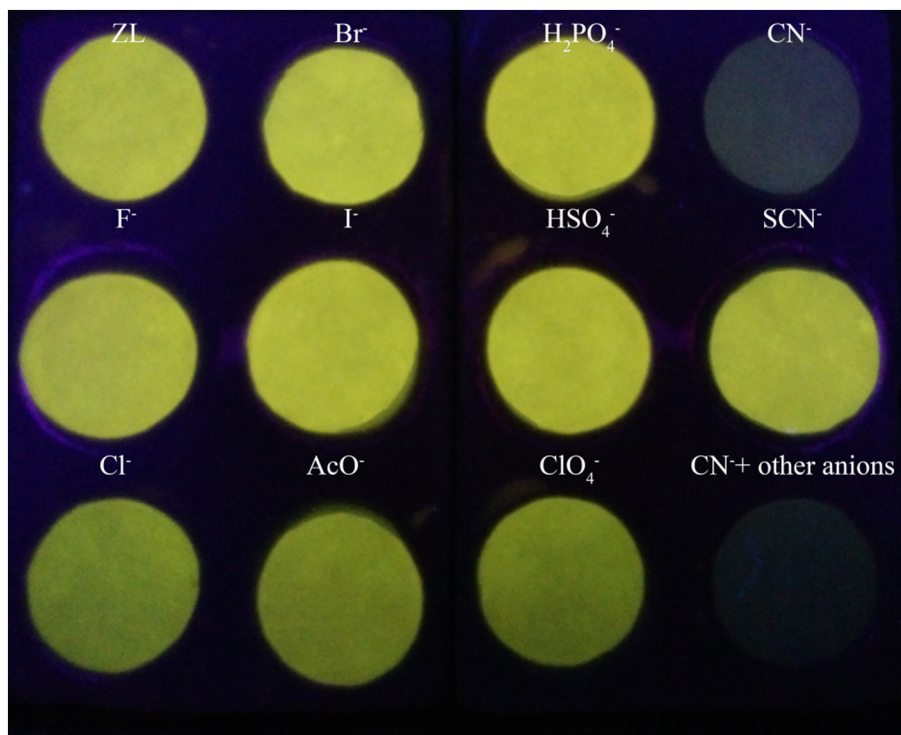


Fig. 14. Photographs of ZL and the mixture of ZL and different anions on the test papers in the DMSO/H₂O (7:3, v/v) solution irradiation at 365 nm.